

Research Article

Assessment of Wind Characteristics and Wind Power Potential of Gharo, Pakistan

Zahid Hussain Hulio 

Department of Industrial Engineering and Management, Dawood University of Engineering and Technology, Karachi, Pakistan

Correspondence should be addressed to Zahid Hussain Hulio; zahidhussain@163.com

Received 28 December 2019; Revised 5 December 2020; Accepted 18 January 2021; Published 16 February 2021

Academic Editor: Abhijeet P. Borole

Copyright © 2021 Zahid Hussain Hulio. This is an open access article distributed under the Creative Commons Attribution License, which permits unrestricted use, distribution, and reproduction in any medium, provided the original work is properly cited.

The objective of this research work is to assess the wind characteristics and wind power potential of Gharo site. The wind parameters of the site have been used to calculate the wind power density, annual energy yield, and capacity factors at 10, 30, and 50 m. The wind frequency distribution including seasonal as well as percentage of seasonal frequency distribution has been investigated to determine accurately the wind power of the site. The coefficient of variation is calculated at three different heights. Also, economic assessment per kWh of energy has been carried out. The site-specific annual mean wind speeds were 6.89, 5.85, and 3.85 m/s at 50, 30, and 10 m heights with corresponding standard deviations of 2.946, 2.489, and 2.040. The mean values of the Weibull k parameter are estimated as 2.946, 2.489, and 2.040 while those of scale parameter are estimated as 7.634, 6.465, and 4.180 m/s at 50, 30, and 10 m, respectively. The respective mean wind power and energy density values are found to be 118.3, 92.20, and 46.10 W/m² and 1036.6, 807.90, and 402.60 kWh/m². As per cost estimation of wind turbines, the wind turbine WT-C has the lowest cost of US\$ Cents 0.0346/kWh and highest capacity factors of 0.3278 (32.78%). Wind turbine WT-C is recommended for this site for the wind farm deployment due to high energy generation and minimum price of energy. The results show the appropriateness of the methodology for assessing the wind speed and economic assessment at the lowest price of energy.

1. Introduction

The United Nations General Assembly (UNGA) in the year 2015 provided a powerful mechanism for an international corporation on sustainable development goals (SGD'S) of Earth. The agenda 2030 comprises three important facets including decreasing poverty, right full distribution of resources and justice, and sustainable energy and environment of the planet. On the face of it, the green energy was central to an agenda that focuses on reliable, affordable, and accessible energy to all. The overall objective of UNGA to meet the future energy demands via renewable energy is achievable while minimizing the impact of dangerous environment.

In recent years, the rising trend of electricity generation by renewable energy is taking a positive way all over the world. Owing to growth of renewable energy resource, the wind energy generation is ahead of all natural resources. There are some noteworthy reasons that played constructive

role in development of wind energy generation including atmosphere, state-of-the-art design of wind turbines, and low cost/kWh. Wind is a natural and irregular source of energy that somewhat makes it less efficient than the conventional sources of energy. However, the conventional sources of energy have some issues too. The changing price of oil in world markets and climate contamination is making it less favourable for generation of energy. More specifically, the less developing world is facing severe socioeconomic problems. Pakistan is also facing similar problems of energy generation with fossil fuels.

Energy generation in Pakistan is mainly achieved through the conventional resources. This is a costly business for Pakistan owing to import of the costly oil. The rise in oil prices in international market can put a huge pressure on the country to increase the prices of oil. The oil import statistics showed a rising trend at 3.8% since last two decades. During 1990 to 2014, the oil consumption increased from 28.6–67

MTOE (million tons of oil equivalent) [1]. The overall consumption of oil and gas accounted for 72%. Around 65% of energy generation is being materialized by burning the crude oil. Owing to increased use, natural gas has started to deplete. Also, energy shortages are a major cause of loss of GDP (2%) during the last decade [1]. During the year 2015-16, 111,300 GWh electricity was generated against the demand of 106,966 GWh in 2014-15 [2]. However, the consumption increased from 85,818 GWh to 90,431 GWh during last year. Pakistan has around 9.06% appropriate land area of the total which can be utilized for the development of wind farms [3].

The Government of Pakistan in the year 2004 constituted the Alternate Energy Development Board (AEDB) to assess the natural resource and install the renewable energy power plants. The major cause behind the formation of AEDB was the rapid rise of prices of oil. This led to the foundation of renewable energy policy formulation and assessment of wind energy, biomass, and small hydro and solar resource assessment and later led to the installation of the wind mast throughout the country. In this regard, the external expert institutions including National Renewable Energy Laboratories helped to prepare wind mapping of Pakistan. Also, indigenous institutions like Pakistan Meteorological Department (PMD) installed wind masts at different locations of Pakistan. The geographical wind mapping and intensity at 80 m is given in Figure 1. The surface roughness length of Pakistan is given in Figure 2.

The wind characteristics including speed, direction, and temperature of Kiribati were investigated in [6] in which the researchers used the Weibull parameters and found the moment method (MM) to be the accurate method. In another research work, the wind characteristics and power potential of Nooriabad (Pakistan) were investigated in [7], in which the researchers applied five methods to achieve the accuracy of Weibull parameters. The wind power potential assessment of Lithuania was examined by [8]. The authors used Weibull probability distribution function to assess the wind resource. For Chad located in North-Central Africa, the wind resource assessment has been carried out at 10 m in which the authors used the Weibull probability function [9].

The continuous published research works are showing the importance of regional development of wind energy potential. Here are some of the mentioned regional studies that are showing the progress in the field of wind energy. The wind potential of Shaharbak city in Kaman province of Iran was assessed by [10]. In another resource study by [11], the author assessed the wind power potential at 10, 20, and 40 m of Yazd province, Iran. Also, another resource assessment of Iran was carried out to determine the energy potential. The considered region was the capital of Iran, Tehran. The energy potential was based on the eleven-year wind speed records calculated in [12]. The wind energy potential of Zarinah city of Iran was examined in [13], the Binalood wind resource study was investigated at 10, 30, and 40 m in [14], and Semnan province wind resource assessment study was conducted by [15].

Teimourian et al. [16] studied the wind power potential of Lotak and Shandol, Iran. The authors considered the wind measurements at 10, 30, and 40 m above the ground level based

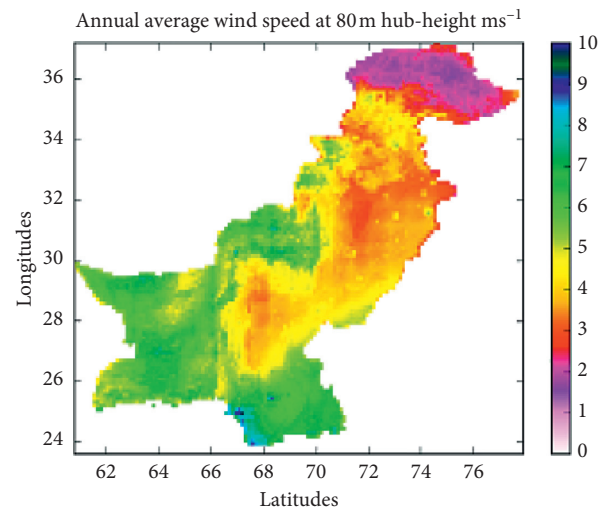


FIGURE 1: Pakistan geographical wind resource assessments at 80 m height [4].

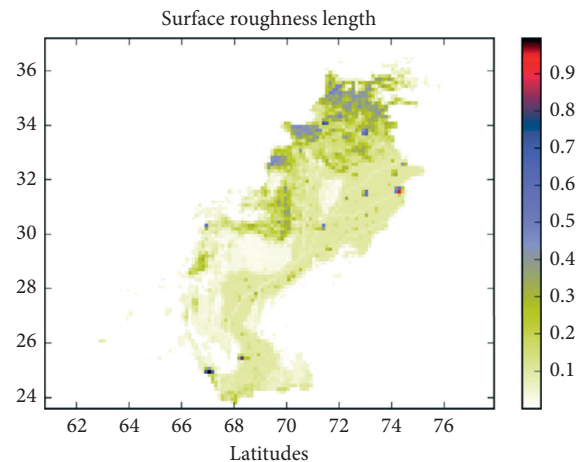


FIGURE 2: Geographical surface roughness length factor of Pakistan [5].

on 10-minute interval of wind measurement and concluded that sites are suitable for power generation at the lowest cost. The wind resource assessment of Turkmenistan has been assessed by Bahrami, Arian. The author assessed wind power potential of 18 different locations and concluded that energy can be generated at the lowest cost [17]. In another research work, Bahrami Arian et al. studied the wind power potential of 17 different locations of Uzbekistan. The author evaluated annual wind power density, energy density, and capacity factor and concluded that Nukus, Kungrad, Ak Bajtal, and Buhara are the best sites for generation of energy at lowest cost [18].

The wind assessment of Jubail city, Saudi Arabia, using the 24 hourly data wind measurements at three different heights was investigated in [19]. The authors used the Weibull distribution function. Similarly, in another work carried out in the aforementioned region of Jubail, the authors took wind measurements of seven locations and investigated the k and c Weibull parameters by means of maximum likelihood, least square regression, and WAsP algorithms [20]. For selection of

best possible site to install wind power plant, the authors used multicriteria decision approach (MCDA) and geographic information system (GIS) in [21]. The wind characteristics of Jeddah, Saudi Arabia, were investigated in [22]. Similarly, the wind resource assessment study for an industrial city of Yanbu, Saudi Arabia, is carried out in [23], as well as for seven different stations of Eastern province of Saudi Arabia, it is carried out in [24], and Lidar-based wind measurements are carried out in [25]. There are also some more wind potential studies of Saudi Arabia has been carried out to assess the wind energy potential considering different wind turbines [26, 27].

The existing rate of potential wind speed of a site is a key factor for realizing the wind energy. Apparently, it is supposed that the wind speeds between 3–25 m/s are conducive for the conversion of wind to energy. Furthermore, the occurrences of the effective wind speeds exhibit the available rate of energy resource. The valuation of wind power using the seasonal and diurnal numbers of Waterloo of Canada was carried out in [28]. Similarly, the wind power potential assessment of Borj Cedria in Tunisia was assessed by [29] at 10, 20, and 30 m heights in which the authors projected the wind energy density by assessing the seasonal wind speeds. Also, the wind power potential of five cities including Tangier, Tetuan, Al Hoceima, Nador, and Larach of Northern Morocco was investigated by [30]. The wind characteristics of Port Said in Egypt [31] were used to investigate the energy arena. The authors used the energy flux method. The measured wind speed data were used for Tindouf in [32], which considered the eight-year data, and for Timimoun region of Algeria in [33].

The wind parameters of South Banat constituency of Serbia were investigated by [34]. The authors considered the wind speed data at 10, 40, 50, and 60 m measurement heights and analysed the measured wind speed, direction, and energy density of the site. Furthermore, there are number of wind resource assessment studies available in the literature carried out at diverse parts of world including Korea [35], China [36], Malaysia [37], India [38], Egypt [39], Pakistan [7, 40, 41], and Columbia [42].

In this paper, an analysis of wind characteristics is carried out to assess the wind energy potential of Gharo site. The measured wind speeds at 10, 30, and 50 m are analysed to assess the wind power prospective of the mentioned site. The wind frequency distribution including seasonal wind frequency and percentage of wind frequency has been examined to determine the accurate wind power potential of the site. In this paper, the applications of Weibull distribution function for the estimation of wind energy resource assessment of Gharo have been carried out. The annual wind power density, wind energy, and capacity factors are calculated at the three measured heights. Also, the economic assessment of the site has been assessed to check the viability of energy yield from suggested wind turbines at the lowest cost (US\$/kWh).

2. Methodology and Data

2.1. Geographical Features of Site. The small town of Gharo is geographically located in Thatta district, Sindh province, Pakistan. The Gharo wind mast is situated in the peripheries

of the town. The geographical view of site is shown in Figure 3. The measured wind speeds were taken at three heights: 10, 30, and 50 m. The meteorology mast is equipped with NRG data acquisition system. Table 1 shows the specifications of the atmospheric sensors. The topographical location of the site is 24°35'48"N and 67°26'39"E. Table 2 shows the site-specific surface roughness values. This site can easily host the future wind farm projects. The Government of Pakistan is taking keen interest in the development of wind energy, and it established the Alternate Energy Development Board (AEDB). Also, some prescribed standards have been set by the international wind energy forum. The standards set by NREL provide the essential insights of wind energy generation and classification that is given in Table 3, and the wind turbine design standards by International Electrotechnical Commission (IEC) corresponding to the site are given in Table 3.

2.2. Wind Power Classification and IEC Turbine Classes.

To simplify the wind power density, the wind resource is divided into seven wind classes. The wind class division is basically based on energy generated from a particular wind speed. Table 4 shows the classification of wind energy generation by National Renewable Energy Laboratories. Apparently, the wind classes above 4 are generally considered as feasible for installing the wind power plants. It provides two essentials including flow of wind speed and economics of energy being generated from wind speed. Wind classes 1 and 2 are generally not considered feasible for the wind power generation. The wind energy classes also provide necessary framework for economic viability of wind turbines. The wind turbine classes are given in Table 3 under which the wind turbines are manufactured by different makers. Table 3 provides the significant manufacturing framework for the wind turbines as suggested by the International Electrotechnical Commission (IEC-61400). Similarly, the typical values of surface roughness length and power law exponent are given in Table 2.

2.3. Assessment of Wind Data. Wind is a referred as development of air in atmosphere. It is a highly changing atmospheric parameter that changes with respect to time. It is generally accepted that the wind speed variation is better calculated using probability density function. The methodology mapping of wind resource assessment of Gharo site is given in Figure 4.

2.4. Assessment of Wind Shear

2.4.1. Log Law. While considering the atmosphere, the turbulent mix can be taken in a similar way to molecular mixing. Also, this is known as k theory. Let suppose the turbulent mixing comprising of shear forces can be derived from relationship of wind speed which is given in the following equation:

$$u = \frac{U_*}{k} \ln\left(\frac{Z - D}{Z_0}\right), \quad (1)$$



FIGURE 3: Geographical location of wind site Gharo.

TABLE 1: Technical parameters of the installed atmospheric sensors.

	Wind speed sensor	Temperature sensor
Sensors	Cup type (M# 40)	6 - ICT radiation plate (M # 110)
Operative assortment	1-90 m/s	-40~52.5 °C
Correctness	±0.8%	±1.1°C
Temperature assortment	-55~60°C	-40~52.5°C
Distance constant	3.0 m	—
Display assortment	0-120 Hz	0~2.5 V DC
Weight	0.2 kg	0.5 kg

TABLE 2: Typical values of surface roughness length and power law exponent.

Terrain	Z_0	α
Ice, mud flat	$10^{-3} \sim 3 \cdot 10^{-3}$	—
Calm sea	$2 \cdot 10^{-4} \sim 3 \cdot 10^{-4}$	—
Sand	$2 \cdot 10^{-4} \sim 10^{-3}$	0.01
Mown grass	0.001~0.01	—
Low grass	0.01~0.04	0.13
Fallow field	0.02~0.03	—
High grass	0.04~0.1	0.19
Forest and wood land	0.1~1	—
Suburb or built area	1~2	0.32
Town, city	1~4	—

TABLE 3: IEC-specified wind turbine classes [43].

Wind turbine class	I	II	III	S
V_{ref} (m/s)	50	42.5	37.5	
AI_{ref}	—	0.16	—	Values specified by designer
BI_{ref}	—	0.14	—	
CI_{ref}	—	0.12	—	

where U is the friction, k is the von Karman constant, Z_0 is the roughness length, and D is the displacement height.

The wind speed is computed for a reference height is expressed in the following equation:

$$\frac{U}{U_R} = \left(\frac{\ln(Z/Z_0)}{\ln(Z_R/Z_0)} \right), \quad (2)$$

where U_R refers to wind speed at the reference height Z_R .

2.4.2. Power Law. Generally, power law refers to increase in wind speed with height owing easier evaluation. It can be expressed as

$$\frac{U}{U_R} = \left(\frac{(Z-D)}{Z_R} \right)^\alpha, \quad (3)$$

where α is the power law exponent.

The power law exponent can be between 0.1 to 0.32 depending upon the landscape of the site. The exponent can be calculated from the roughness length.

$$\alpha = \frac{\ln(\ln(Z/Z_0)/(Z_R/Z_0))}{\ln(Z/Z_R)} \approx \frac{1}{\ln \sqrt{(Z \cdot Z_R)/Z_0}} \quad (4)$$

2.4.3. Weibull Probability Distribution Function. The Weibull distribution function is used to achieve the effectiveness of wind potential. The probability density function $f(V)$ and cumulative distribution function are given as follows [7, 44]:

$$f(V) = \left(\frac{k}{c} \right) \left(\frac{V}{c} \right)^{k-1} \exp \left[- \left(\frac{V}{c} \right)^k \right], \quad (5)$$

$$F(V) = 1 - \exp \left[- \left(\frac{V}{c} \right)^k \right].$$

Rayleigh distribution is a diverse practice of Weibull distribution function. In such instance, the value of k parameter is considered as 2. The probability and cumulative distribution functions are given as follows [45, 46]:

TABLE 4: Wind energy generation classification by National Renewable Energy Laboratories [43].

Wind class	Resource	Height 30 m (AGL)		Height 50 m (AGL)	
		Wind speed (m/s)	Wind power density (W/m ²)	Wind speed (m/s)	Wind power density (W/m ²)
1	Poor	00–5.1	0–160	00–5.4	00–200
2	Marginal	5.1–5.9	16–240	5.4–6.2	200–300
3	Moderate	5.9–6.5	240–320	6.2–6.9	300–400
4	Good	6.5–7.0	320–400	6.9–7.4	400–500
5	Excellent	7.0–7.4	400–480	7.4–7.8	500–600
6	Excellent	7.4–8.2	480–640	7.8–8.6	600–800
7	Excellent	8.2–11.0	640–1600	>8.6	>800

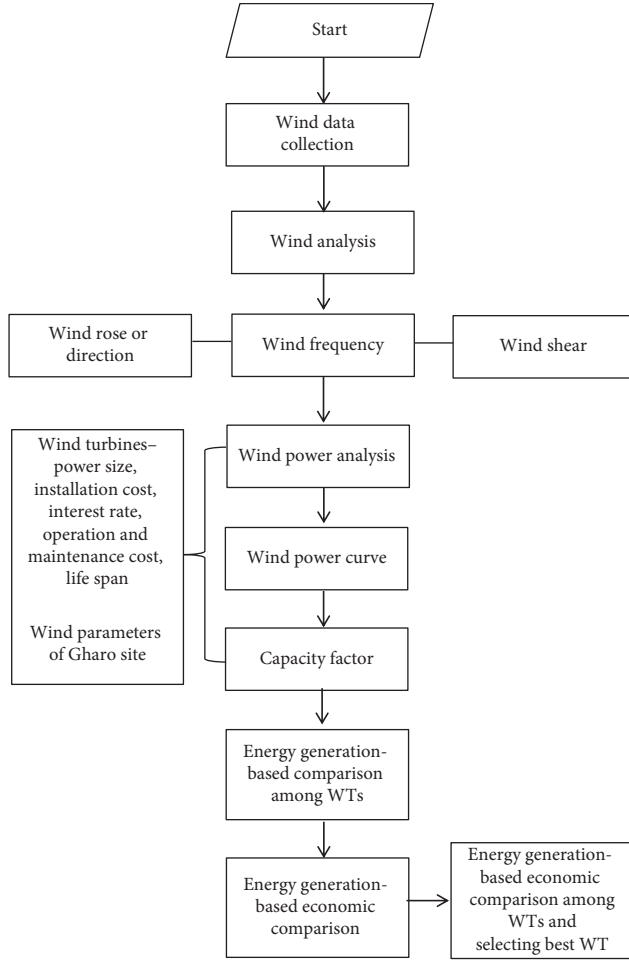


FIGURE 4: Methodology mapping of wind resource assessment of Gharo site.

$$f(V) = \frac{\pi}{2} \left(\frac{V}{V_{avg}} \right) \exp \left[- \left(\frac{\pi}{4} \right) \left(\frac{V}{V_{avg}} \right)^2 \right], \quad (6)$$

$$F(V) = 1 - \exp \left[- \left(\frac{\pi}{4} \right) \left(\frac{V}{V_{avg}} \right)^2 \right].$$

The average wind speed V_{avg} is mathematically expressed as follows [44]:

$$V_{avg} = \frac{1}{N} \sum_{i=1}^N V_i. \quad (7)$$

The variance and standard deviation are expressed as follows:

$$\sigma^2 = \frac{1}{N-1} \sum_{i=1}^N (V_i - V_{avg})^2, \quad (8)$$

$$\sigma = \sqrt{\frac{1}{N-1} \sum_{i=1}^N (V_i - V_{avg})^2}.$$

By using Weibull parameters, the mean and variance of wind speed can expressed as [12]

$$V_{avg} = c \Gamma \left(1 + \frac{1}{k} \right), \quad (9)$$

$$\sigma^2 = c^2 \left[\Gamma \left(1 + \frac{2}{k} \right) - \Gamma^2 \left(1 + \frac{1}{k} \right) \right],$$

where Γ refers to gamma function and can be represented as

$$\Gamma_x = \int_0^{\infty} e^{-u} u^{x-1} du. \quad (10)$$

2.5. Assessment of Coefficient of Variation. The coefficient of variation of wind speed is calculated by the following equation [47]:

$$C_V = \frac{\sigma}{\bar{x}} \quad (11)$$

2.6. Wind Power Density. The wind power density W_P is mathematically described as [48]

$$W_P = \frac{1}{2} \rho A_T V^3, \quad (12)$$

where V is the wind speed; ρ is the air density; and A_T is the rotor area of the wind turbine. The Betz number is denoted by C_p and can be referred to as [49]

$$W_p = \frac{1}{2} \rho C_p A_T V^3. \quad (13)$$

The wind power density (W_{pd}) obtained from equation (11) is given as follows:

$$W_{pd} = \frac{P}{A} = \frac{1}{2} \rho C_p V^3. \quad (14)$$

W_{pd} with Weibull pdf is expressed as [50]

$$W_{pd} = \frac{P}{A_T} = \frac{1}{2} \rho V^3 \Gamma \left(1 + \frac{3}{k} \right). \quad (15)$$

The energy is obtained by the wind machine and is calculated as follows. While substituting equation (2) in equation below, equation (16) can be read as

$$E = T \int_0^{\infty} P(V) f(V) dV, \quad (16)$$

$$E = T \int_0^{\infty} \left(\frac{k}{c} \right) \left(\frac{V}{c} \right)^{k-1} \exp \left[- \left(\frac{V}{c} \right)^k \right] P(V) d(V).$$

2.7. Capacity Factor. The capacity factor is stated as

$$C_f = \frac{\text{ActualPower (Ap)}}{\text{RatedPower (Rp)}}. \quad (17)$$

3. Results and Discussion

In this paper, the wind characteristics and power assessment of Gharo site have been studied. The site is located in wind corridor (Gharo-Ketti-Bunder) of Pakistan. The small town is located in Thatta district of province of Sindh, Pakistan. According to census department of Pakistan, there were 2,000 families living in Gharo in 2017. The wind measurements taken at 10, 30, and 50 m are examined in this paper for a period of one year. Further, the results of wind resource assessment and power assessment are discussed below in the coming sections.

3.1. Assessment of Surface Roughness Factor Z_0 and Power Law.

The power law exponent varies between the two measurement heights. The power law is checked carefully because it does not have physical representation of surface layer and does not explain the flow near to the ground. Both log law and power law generally explain the wind profile of the site. The maximum and minimum values of Gharo site are given in Table 5.

3.2. Diurnal Wind Variation of Site. Figures 5(a)–5(c) show the seasonal diurnal wind speed variations at Gharo site over a period of year at three heights 10, 30, and 50 m. The objective of assessment of hourly mean diurnal wind variation is to determine the seasonal variation of the site at 10, 30, and 50 m. It is observed from the results that wind speed

TABLE 5: Maximum and minimum values of Z_0 .

	Max	Min	Mean
Z_0	4.9	0.44	2.298

is lower during the night, whereas wind speed after sunrise picks up and levels maximum at the evening time during 4:00 pm to 5:00 pm at 30 and 50 m. It again starts to decrease as time passes to night. The visible maximum number was found in the months of March, May, June, and August at the height of 10 m. Similarly, the nature of trends is also visible in the months of March, May, June, and August at the height of 30 m. At 50 m, the maximum values are found to be in March, May, June, and August. The seasonal diurnal wind variation has been found maximum from 00:00–05:00 hours and again from 11:00–18:00 during 24 hours of a day for a period of one year. Similar trends of diurnal wind speed variation can be seen at 10, 30, and 50 m. Figures 5(a)–5(c) show the diurnal wind speed variation of site at 10, 30, and 50 m for a period of one year.

3.3. Monthly Temperature of Site. Figure 6 shows the monthly mean temperature of Gharo site at 50, 30, and 10 m heights. Higher values of temperature were observed to be in the months of summer, whereas lower values were observed in winter. The mean values of temperature are found to be 24.80, 24.84, and 24.98 at 50, 30, and 10 m heights.

3.4. Wind Speed Frequency Distribution. In other words, the wind speed frequency distribution can be plotted by different wind bins against their relative frequencies. There are two important methods including data bins of site and frequency of wind speed of site for obtaining the necessary frequency distribution.

3.4.1. Data Bins. The assortment of the data into narrower level of wind speed bands is termed as the binning of the data. In this research, the width of bin is 1 m/s. For example, a measured wind speed of 3.5 m/s is placed in $3 < X \leq 4$ m/s bin. However, the value of each bin is 0.5 m/s, and 1.5 m/s is used in the calculations and in frequency distribution.

3.4.2. Relative Frequency. The relative frequency is proportional to wind speed in each bin. The relative frequency can be viewed as the estimate of probability of given wind speed in the bin. The relative frequency can be described as follows:

$$\text{relative frequency} = P(V_i) = \frac{\text{frequency of given wind speed}}{\text{total period}}$$

Figure 7 shows the annual cumulative frequency distribution of wind speed at three heights including 10, 30, and 50 m. It is clear from Figure 7 that the values of wind speed are greater than 5 m/s for a period of 6280 hours at 30 m. Similarly, the values of wind speed are greater than 5 m/s at

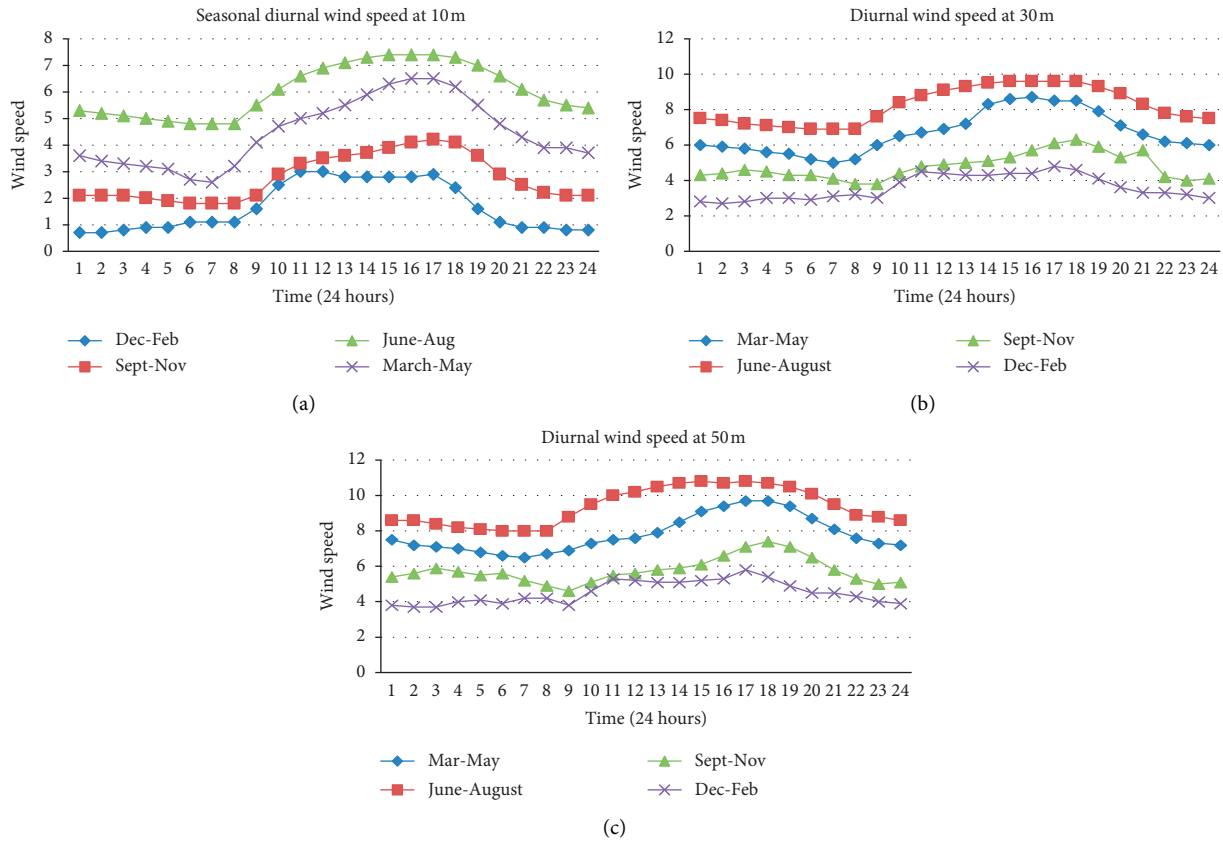


FIGURE 5: Diurnal wind speed variation at 10, 30, and 50 m above the ground level (AGL).

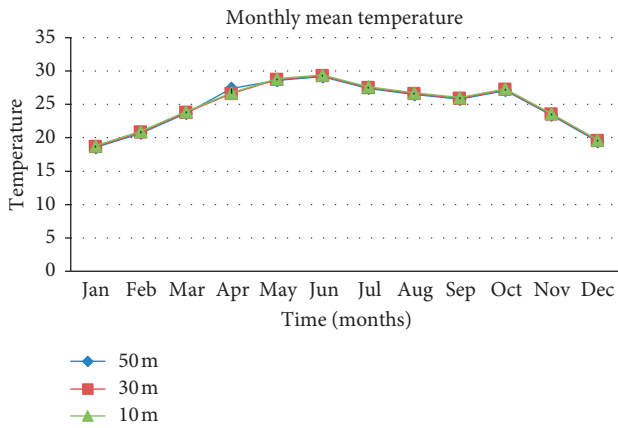


FIGURE 6: Monthly mean temperature of Gharo site at 50, 30, and 10 m heights.

50 m for a period of 6852 hours. The site assessment showed that there is enough wind to generate the energy.

Figure 8 shows the annual wind frequency distribution of Gharo site at 10, 30, and 50 m heights. It is clear from Figure 8 that during 730 hours, wind speed is 5 m/s, during 710 hours, wind speed is 6 m/s, during 1015 hours, wind speed is 7 m/s, during 1025 hours, wind speed is 8 m/s, during 790 hours, wind speed is 9 m/s, during 740 hours, wind speed is 10 m/s, and so forth at 50 m. This analysis of

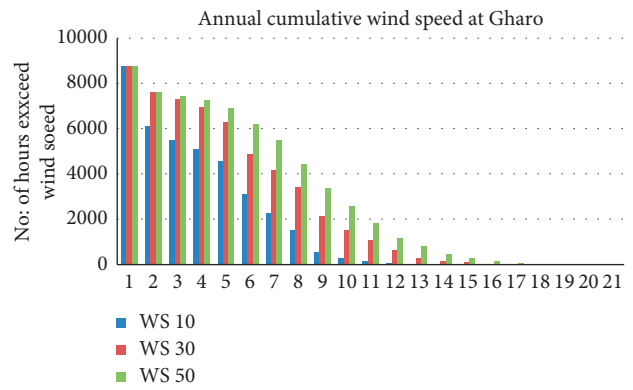


FIGURE 7: Annual cumulative frequency distribution of wind speed at Gharo site.

measured site shows that the wind potential can be used for the installation of utility wind turbines.

Figure 9 shows the percentage (%) of frequency of wind speed of Gharo site. At maximum height (50 m) of measured site, we observed that the wind speed at 85% accounts for 5 m/s, that at 8% accounts for 6 m/s, that at 12% accounts for 8 m/s, and that at 9% accounts for 9 m/s. However, the measured site observation is different at three heights. The wind speed 5 m/s is observed to be 16%, 7 m/s is 8%, and 8 m/s is 15%. This indicates that the wind

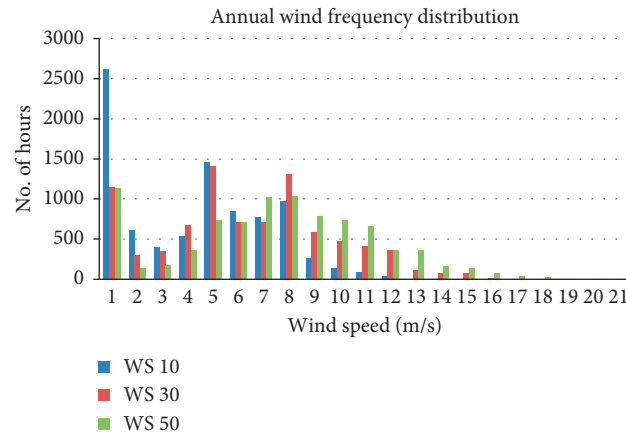


FIGURE 8: Annual wind frequency distribution of Gharo site.

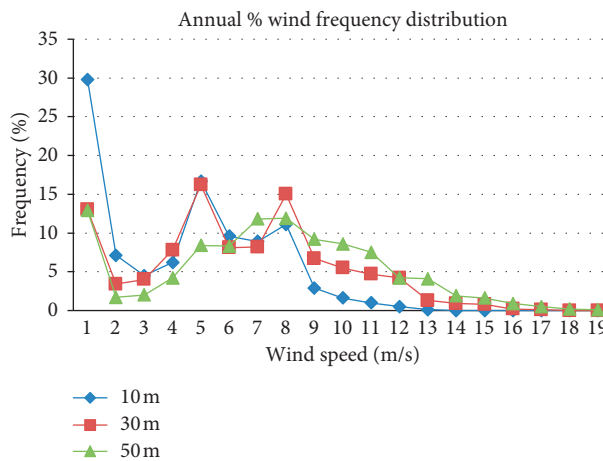


FIGURE 9: Annual % of wind frequency distribution.

energy can be generated from the prevailing wind speed of Gharo site.

3.5. Seasonal Analysis of Wind Frequency Distribution.

Figures 10(a)–10(d) present the seasonal wind frequency distribution for a period of one year. Figure 10(a) shows the wind distribution for a spring season that starts from March and lasts up to May. It can be observed from Figure 10(a) that the wind speed reached 5 m/s, 6 m/s, 7 m/s, 8 m/s, 9 m/s, 10 m/s, and 11 m/s for a period of 330 hours, 213 hours, 212 hours, 371 hours, 185 hours, 137 hours, and 142 hours, respectively, at 30 m. Similarly, the wind speed reached 5 m/s, 6 m/s, 7 m/s, 8 m/s, 9 m/s, 10 m/s, 11 m/s, 12 m/s, and 13 m/s for a period of 138 hours, 187 hours, 261 hours, 296 hours, 228 hours, 230 hours, 191 hours, 99 hours, and 110 hours, respectively, at 50 m. The observed wind speed measurement shows the increase with respect to increase in height.

Figure 10(b) shows the wind speed for a summer season. The summer season starts from the month of June and lasts up to August. The seasonal wind speed frequency showed that the wind speed reached 5 m/s, 6 m/s, 7 m/s, 8 m/s, 9 m/s,

10 m/s, 11 m/s, and 12 m/s for a period of 170 hours, 162 hours, 210 hours, 496 hours, 255 hours, 238 hours, 206 hours, and 230 hours, respectively, at 30 m. The observed wind speed measurement showed the strong presence of wind at 30 m. Similarly, the wind speed reached 5 m/s, 6 m/s, 7 m/s, 8 m/s, 9 m/s, 10 m/s, 11 m/s, 12 m/s, 13 m/s, and 14 m/s for a period of 21 hours, 64 hours, 112 hours, 198 hours, 265 hours, 277 hours, 280 hours, 305 hours, 198 hours, and 200 hours, respectively, at 50 m.

Figure 10(c) shows the wind frequency distribution during the period for autumn season that starts from September and lasts up to November. The measured observations showed that the 5 m/s wind speed lasts up to 435 hours, 6 m/s wind speed for 170 hours, 7 m/s wind speed for 160 hours, 8 m/s wind speed for 280 hours, and for 9 m/s is reaches to 110 hours at the height of 30 m. Similarly, for the measurement height of 50 m, the wind speed for 5 m/s is rests up to 61 hours, 6 m/s wind speed for 125 hours, 7 m/s is for 250 hours, 8 m/s is for 210 hours, 9 m/s is for 290 hours, 10 m/s is for 255 hours, and 11 m/s wind speed for 175 hours.

Figure 10(d) is showing the seasonal wind speed for winter season. The wind speed reached 5 m/s, 6 m/s, 7 m/s, and 8 m/s for a period of 475 hours, 170 hours, 135 hours, and 160 hours, respectively, at 30 m. Similarly, the wind speed reached 5 m/s, 6 m/s, 7 m/s, 8 m/s, 9 m/s, and 10 m/s for a period of 66 hours, 76 hours, 155 hours, 280 hours, 208 hours, and 280 hours, respectively, at 50 m.

Similarly, the wind frequency distribution seasonal percentage (%) is given in Figures 10(a)–10(d) for further detailed analysis of the wind of Gharo site (Figure 11).

3.6. Wind Speed Variation Analysis. The wind data were collected over a period of one year in 2009 and used in the analysis. The wind analysis was carried out at 10, 30, and 50 m heights. The overall mean values of wind speeds along with corresponding standard deviations and k and c parameters at the measurement heights for a period of one year are enumerated in Tables 6–8, respectively. The mean wind speeds are found to be 3.85, 5.85, and 6.89 m/s at 10, 30, and 50 m, respectively, as listed in Table 9. It can be concluded from the measured wind data that wind speed (m/s)

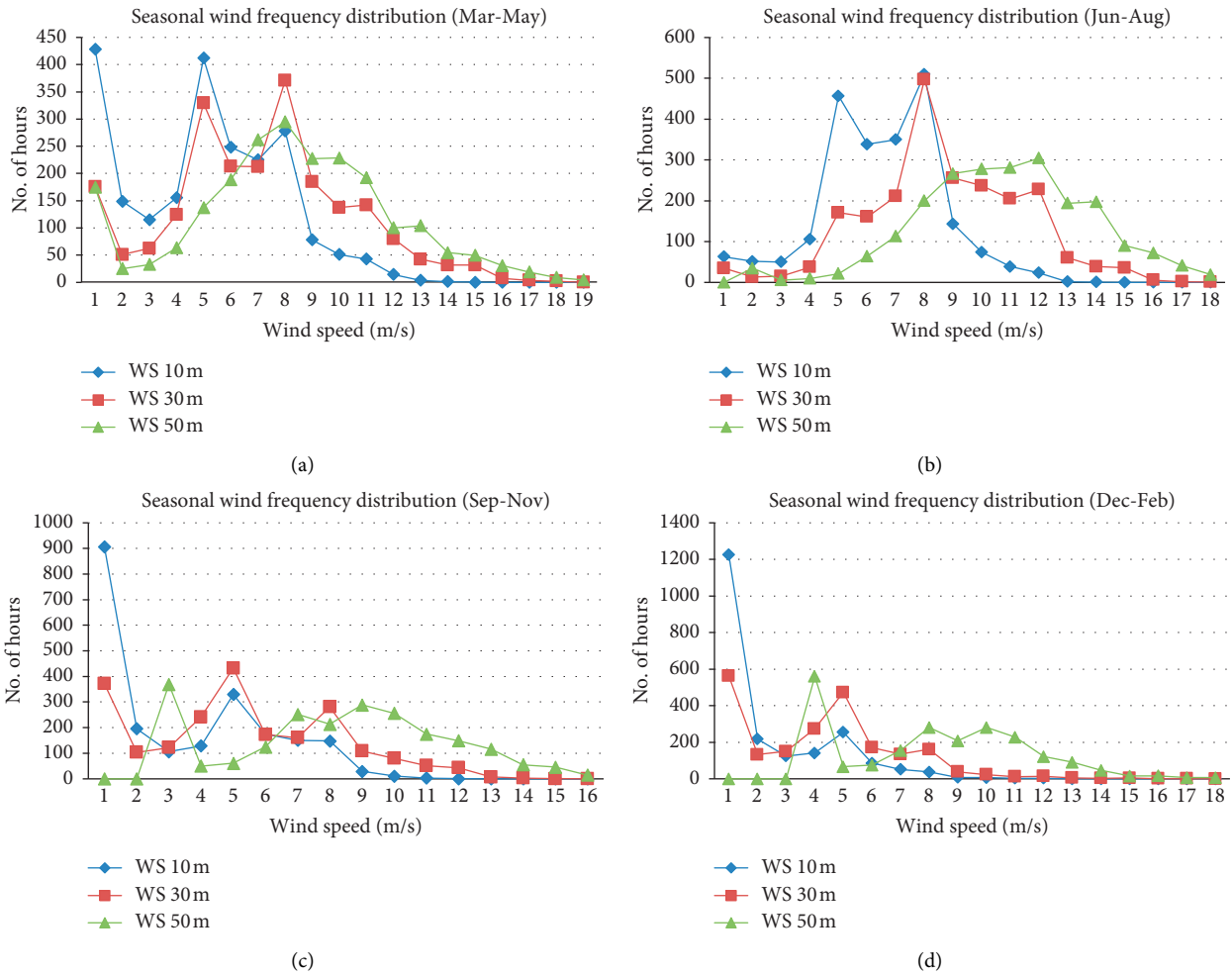


FIGURE 10: Seasonal wind frequency distribution of Gharo site. (a) March–May. (b) June–August. (c) September–November. (d) December–February.

increases with increasing altitude. Figure 12(a) shows the monthly mean variation of wind speed at the three measurement altitudes. Figure 12(a) shows that the higher values of wind speed are found to be in July while lower values of wind speed are found to be in November at three measurement heights. However, Figure 12(b) shows the ten-minute wind measurements of Gharo site. The average seasonal (winter, spring, summer, and autumn) value at 10, 30, and 50 m heights is given in Tables 9–11, respectively. The higher number of wind speeds is observed during the summer season and the lower number of wind speeds is observed during the winter season at all respective measurement heights. The concept of most likely wind speed is used to analyse the wind. The concept of most likely wind speed is used to refer the most occurring values of wind speed in the dataset. Accordingly, the highest values of 7.19, 9.96, and 11.4 m/s of most likely winds are found in July at 10, 30, and 50 m, respectively.

3.7. Wind Rose Graph. For harnessing maximum possible wind energy, the appropriate knowledge of wind direction is significant. This can help to install wind turbine at the best

position. The hourly wind direction is used to find out the predominant wind direction of Gharo site. The rose diagram for a period of one year is given in Figure 13. However, this is obvious from the wind speed direction that the wind blows from almost all directions with larger contribution from southwest and northwest directions.

3.8. Coefficient of Variation. The stability of the wind speed is effective for determining the wind energy of specific site. The average coefficient of variation was found to be 0.49, 0.50, and 0.70 at 50, 30, and 10 m heights, respectively. The maximum variation was found to be 0.78 in December and the minimum variation was 0.22 in July at 50 m. At 30 m, the maximum values were found to be 0.79 in November and the minimum values were found to be 0.23 in July. At 10 m, the maximum values were found to be 1.20 in November and the minimum values were found to be 0.25 in July. The detailed coefficient of variation of wind speed at 50, 30, and 10 m is given in Table 12.

The k and c parameters are used to determine the wind power prospective of Gharo. The values of the c parameter change with time and site similar to the wind speed. A

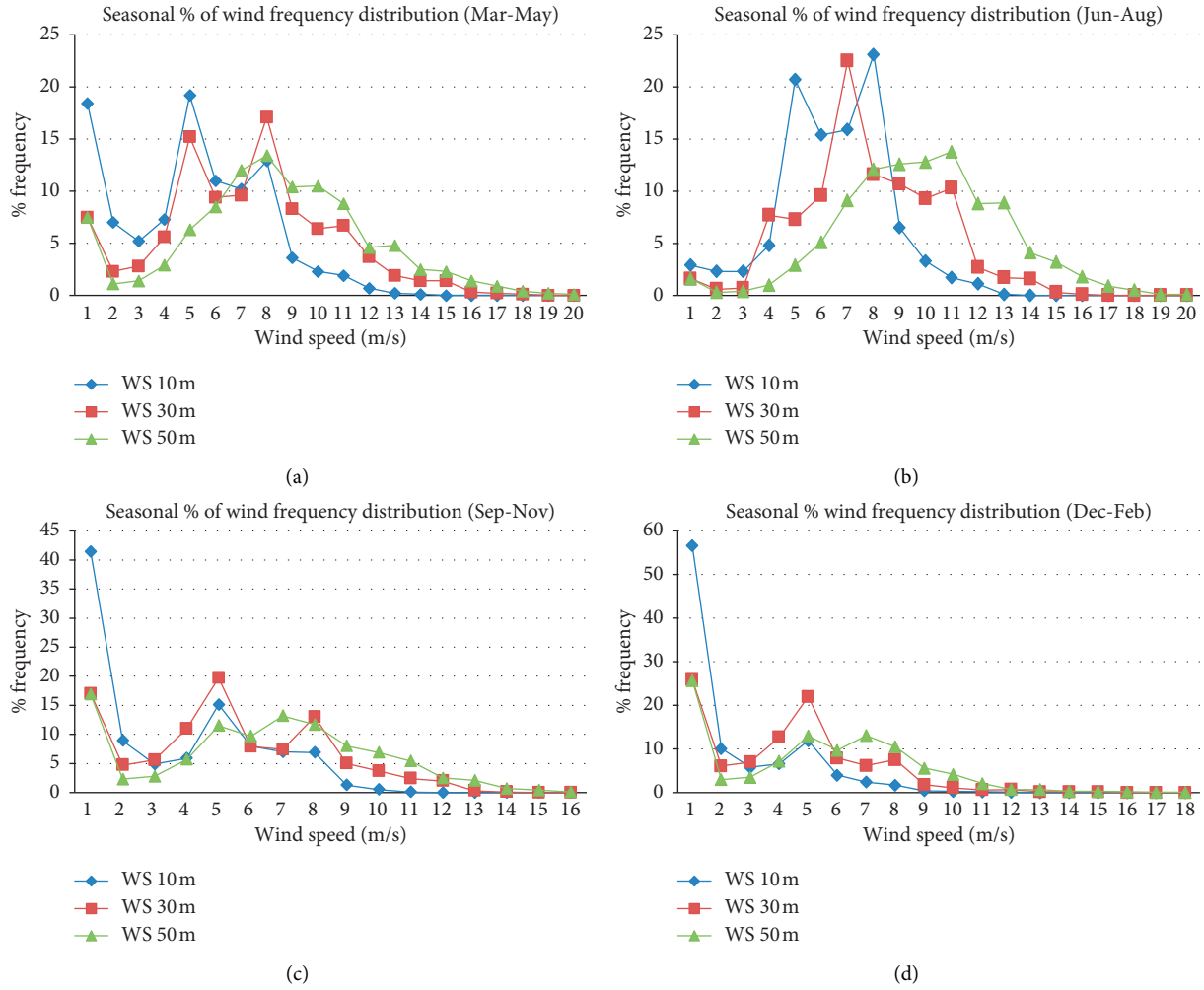


FIGURE 11: Seasonal percentage of wind frequency distribution of Gharo site. (a) March–May. (b) June–August. (c) September–November. (d) December–February.

TABLE 6: Mean wind speed, standard deviation, and Weibull k and c parameters for entire dataset at 50 m.

Month	50 m height			
	Mean	Σ	k	c (m/s)
Jan	4.51	3.16	1.48	5.01
Feb	5.09	3.30	1.62	5.68
Mar	5.10	3.12	1.72	5.74
Apr	7.15	3.27	2.35	8.06
May	10.6	3.02	3.91	11.7
Jun	8.96	2.92	3.42	9.98
Jul	11.4	2.55	5.09	12.4
Aug	7.95	2.60	3.38	8.80
Sep	8.76	2.30	4.25	9.64
Oct	4.75	2.66	1.87	5.40
Nov	3.97	3.11	1.29	4.30
Dec	4.48	3.35	1.40	4.90

TABLE 7: Mean wind speed, standard deviation, and Weibull k and c parameters for entire dataset at 30 m.

Month	30 m height			
	Mean	σ	k	c (m/s)
Jan	3.55	2.50	1.48	3.900
Feb	4.10	2.81	1.60	4.490
Mar	4.22	2.65	1.68	4.680
Apr	6.45	2.40	2.89	7.310
May	9.20	2.80	3.65	10.10
Jun	7.80	2.59	3.30	8.710
Jul	9.96	2.30	4.96	10.82
Aug	6.88	2.35	3.19	7.680
Sep	7.60	2.14	3.98	8.400
Oct	3.82	2.11	1.89	4.200
Nov	3.12	2.50	1.30	3.400
Dec	3.50	2.72	1.29	3.900

number between 1 and 2 of k parameter is indicative of low winds while its increasing trend is indicative of skewness. The obtained average values of k and c parameters were 2.066 and 4.18 m/s at 10 m, 2.600 and 6.465 m/s at 30 m, and 2.648

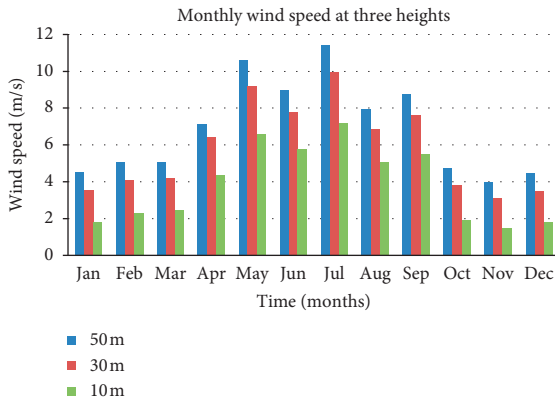
and 7.634 m/s at 50 m. The maximum values and average values of Weibull k and c parameters at 10, 30 and 50 m are given in Tables 4, 5 and 6; respectively. The mean values of c and k parameters are observed to be increasing with

TABLE 8: Mean wind speed, standard deviation, and Weibull k and c parameters for entire dataset at 10 m.

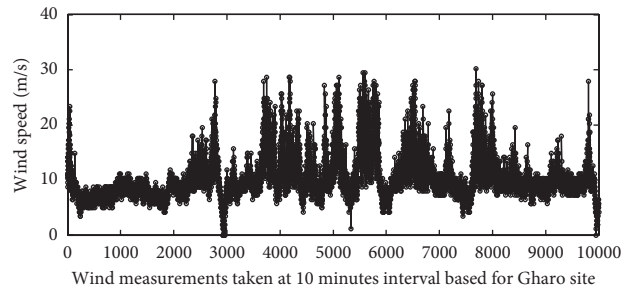
Month	10 m height			
	Mean	σ	k	c (m/s)
Jan	1.80	1.88	1.01	1.79
Feb	2.30	2.28	1.04	2.30
Mar	2.49	2.20	1.16	2.71
Apr	4.36	2.35	1.98	4.90
May	6.59	2.31	3.10	7.36
Jun	5.76	2.10	3.06	6.45
Jul	7.19	1.80	4.66	7.89
Aug	5.10	1.96	2.79	5.70
Sep	5.49	1.89	3.20	6.11
Oct	1.90	1.82	1.02	1.90
Nov	1.49	1.79	0.89	1.35
Dec	1.79	2.10	0.89	1.70

TABLE 9: Mean and maximum wind speed, standard deviation, and Weibull k and c parameters for entire dataset.

Height	Average annual wind speed (m/s)				
	Mean	Maximum	Σ	k	c (m/s)
At 50 m	6.89	11.4	2.946	2.648	7.634
At 30 m	5.85	9.96	2.489	2.600	6.465
At 10 m	3.85	7.19	2.040	2.066	4.180



(a)



(b)

FIGURE 12: Monthly mean wind speed (m/s) of Gharo site at 10, 30, and 50 m height and ten-minute wind measurements of Gharo site.

TABLE 10: Seasonal wind speed, standard deviation, Weibull k and c parameters, and wind power density at 50 m.

At 50	Mean	Σ	k	c (m/s)	W/m^2
Winter	4.693	3.27	1.5	5.196	42.30
Spring	7.616	3.136	2.66	8.500	90.40
Summer	9.503	2.69	3.963	10.39	207.7
Autumn	5.826	2.69	2.470	6.466	132.7

TABLE 11: Seasonal wind speed, standard deviation, Weibull k and c parameters, and wind power density at 30 m.

At 30	Mean	Σ	k	c (m/s)	W/m^2
Winter	3.716	2.676	1.546	4.096	19.00
Spring	6.623	2.616	2.740	7.363	63.00
Summer	8.213	2.413	3.816	9.070	184.0
Autumn	4.846	2.25	2.390	5.333	102.7

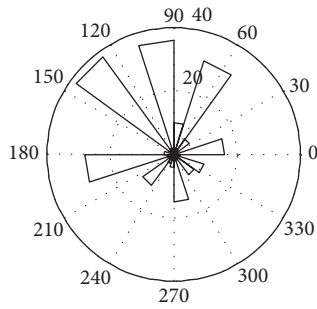


FIGURE 13: Wind rose graph of Gharo site.

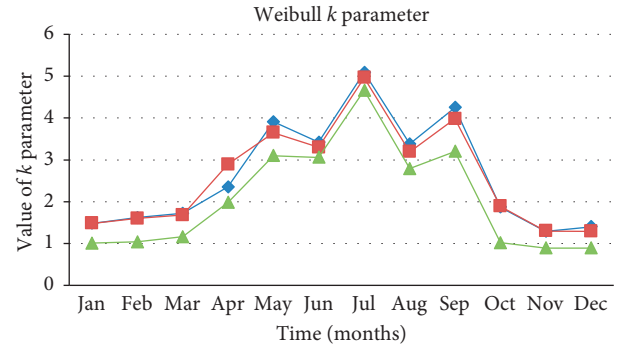
TABLE 12: Coefficient of variation of wind speed at 50, 30, and 10 m for a period of year.

Time (months)	At 50 m	At 30 m	At 10 m
Jan	0.70	0.70	1.04
Feb	0.64	0.68	0.99
Mar	0.61	0.62	0.88
Apr	0.46	0.37	0.54
May	0.28	0.30	0.35
Jun	0.32	0.33	0.36
Jul	0.22	0.23	0.25
Aug	0.32	0.34	0.38
Sep	0.26	0.28	0.34
Oct	0.56	0.55	0.95
Nov	0.78	0.79	1.20
Dec	0.74	0.77	1.17

increasing altitude. Significantly high monthly mean values of shape parameters are seen during July to September, but very low monthly mean values of shape parameters are seen during October to December as shown in Figure 14. The detailed seasonal values of k parameter are given in Tables 10, 11, and 13 corresponding to 50, 30, and 10 heights. However, the higher and lower values of k parameter were observed in summer and winter, respectively.

With reference to scale parameter, the higher values are observed during summer and lower values are observed during winter; the details are given in Tables 10, 11, and 13. A lower value of 5.196, 4.096, and 1.930 m/s is observed in winter season, whereas a higher value of 10.39, 9.070, and 3.503 m/s is observed in summer season at 50, 30, and 10 m, respectively. The mean value of c parameter is found to be 7.634, 6.465, and 4.180 m/s at 50, 30, and 10 m, respectively. Figure 15 shows the monthly detailed c parameter at 50, 30, and 10 m measurement heights.

3.9. Calculations of Wind Power Density and Energy. The calculated values of wind power density and energy density are given in Table 14 at the studied measurement heights. The lower and higher amount of wind power density oscillated from 223–32 W/m², 205–14 W/m², and 138–1 W/m² at 50, 30, and 10 m, respectively. The average amount of wind power density at 50, 30, and 10 m is estimated to be 118.3, 92.2, and 46.08 W/m², respectively. The detailed mean seasonal values of wind power density corresponding to winter, spring, summer, and autumn are given in Tables 10, 11, and 13 at 50, 30, and 10 m. The maximum value of the wind power density is observed during

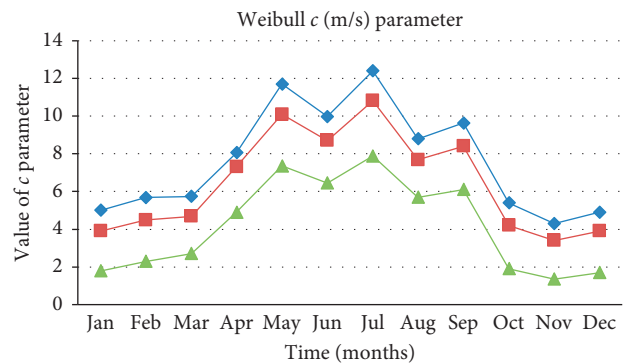


—◆— k at 50 m
—■— k at 30 m
—▲— k at 10 m

FIGURE 14: Weibull k parameters for a period of one year at 10, 30, and 50 m.

TABLE 13: Seasonal wind speed, standard deviation, Weibull k and c parameters, and wind power density at 10 m.

At 10	Mean	Σ	k	c (m/s)	W/m ²
Winter	1.963	2.086	0.980	1.93	1.000
Spring	4.480	2.286	2.080	4.99	18.00
Summer	6.016	1.953	3.503	6.68	115.7
Autumn	2.960	1.833	1.703	3.12	49.70



—◆— c (m/s) at 50 m
—■— c (m/s) at 30 m
—▲— c (m/s) at 10 m

FIGURE 15: Weibull c parameter for a period of one year at 10, 30, and 50 m.

TABLE 14: Wind power density (W/m²) and annual energy density (kWh/m²) for a period of one year.

Height (m)	Power density			Energy density		
	Max	Min	Mean	Max	Min	Mean
50	223	32	118.3	1955	281	1036.6
30	205	14	92.20	1797	123	807.90
10	138	1	46.10	1210	9	402.60

the summer and the minimum value of the wind power density is observed during winter at all measurement heights.

Similarly, the lowest and highest values of energy density ranged from 281 to 1955 kWh/m², 123 to 1797 kWh/m², and 09 to 1210 kWh/m² at 50, 30, and 10 m heights, whereas the mean values of energy density are found to be 1036.9, 807.90, and 402.60 kWh/m² at 50, 30, and 10 m respectively. In general, the higher values of energy density are found in summer and lower values of energy density are found in winter season at all wind measurement heights. The monthly mean variation of wind power density and energy density is depicted in Figures 16 and 17, respectively. Evidently, higher values of both the parameters are seen in summer season and relatively lower values of those are seen in winter season. This means that more energy can be generated in summer time which is also the peak load time due to increased cooling load. Furthermore, the wind power so generated can help in supplementing the peak load demands during summer time and will result in reducing the power generation from fossil fuel.

To estimate the monthly and annual wind energy output at the site, six wind machines of rated capacities of around 2000 to 2750 kW are chosen. Figure 18 shows the power size curves of the turbines. The technical specifications are listed in Table 15. The cut-in speed of a machine is important, and its lower value is indicative of the better performance, in general. In this case, the wind turbines have the minimum cut-in speed which is 3 m/s, and hence it is expected to perform better compared to others. The total annual and monthly energy yields and maximum and minimum capacity factors (CF) obtained using the wind power curves are provided in Tables 16 and 17, respectively. The wind turbine *c* produced the maximum energy of 85133205 kWh with mean CF of 32.75%. However, the wind turbine *E* produced the minimum energy yield of 64860327 kWh during the year with an average CF of 30.91%. Comparatively, wind turbine *C* seems to be more appropriate for the considered site for wind power deployment. Furthermore, the seasonal trend of energy generation is suitable for meeting the local load demand which is expected to be more in summer time.

4. Economic Assessment of Wind Turbines

This section focuses on the assessment of cost of energy generated from wind resources using different types of wind turbines. The objective of this section is to quantify the performance-based price of energy from each type of turbine. The economics of energy can be expressed as [11]

$$\begin{aligned}
 P_{com} &= I \left[\frac{(1 + i_r) - 1}{i(1 + i_r)} \right], \\
 P_{W_{1-t}} &= I \left[1 + n \left\{ \frac{(1 - i_r)^t - 1}{i_r(1 + i_r)^t} \right\} \right], \\
 N_{P_w} &= \frac{P_{W_{1-t}}}{t} = \frac{1}{t} \left[1 + n \left\{ \frac{(1 - i_r)^t - 1}{i_r(1 + i_r)^t} \right\} \right], \\
 T_C &= \frac{P_W}{E},
 \end{aligned}
 \tag{18}$$

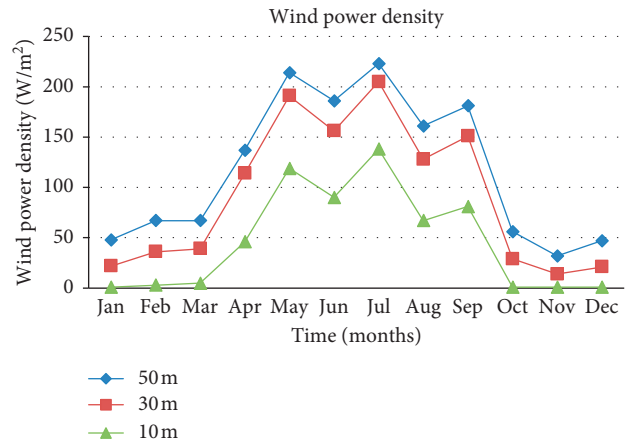


FIGURE 16: Monthly wind power densities (WPD) (W/m²).

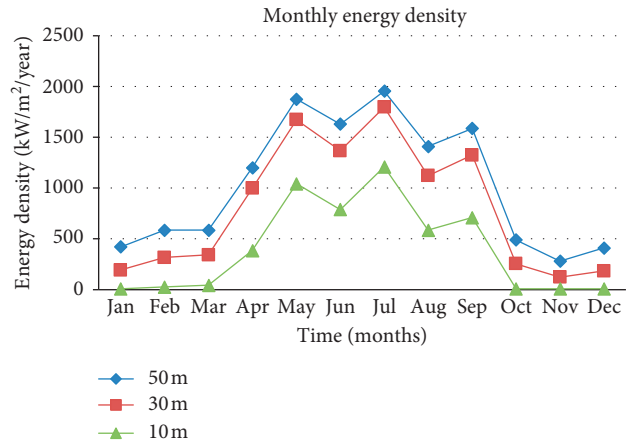


FIGURE 17: Monthly energy density (ED) (kWh/m²).

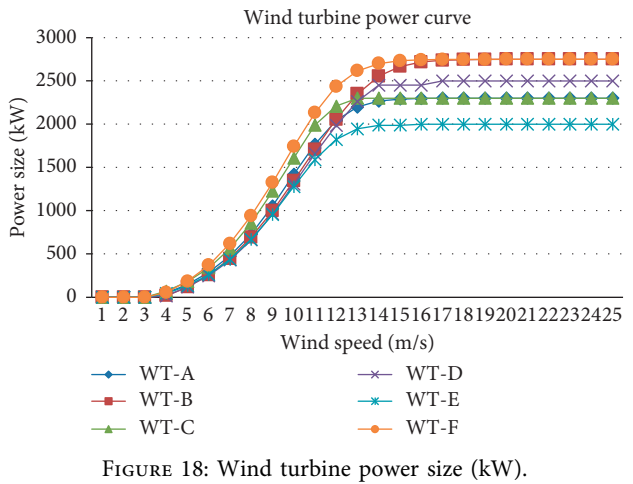


FIGURE 18: Wind turbine power size (kW).

where *E* is energy production and the annual energy yield is computed from equation (19). In equation (19), *T_{ah}* is total hours in a year and *R_p* is rated power of turbine [11]:

TABLE 15: Characteristics of wind turbines.

Wind turbines	Cut-in speed (m/s)	Cut-out speed (m/s)	Rated power (kW)	Rated speed (m/s)	Rotor diameter (m)	Hub height
WT-A	3	25	2300	15	60	60
WT-B	3	25	2750	14	80	60
WT-C	3	25	2300	15	80	80
WT-D	4	25	2500	11.5	60	60
WT-E	4	25	2000	15	80	80
WT-F	3	25	2750	15	92	70

TABLE 16: Wind turbine energy output for a period of one year.

Wind turbine (kWh)	WT-A (2300/82.4)	WT-B (2750/80)	WT-C (2300/90)	WT-D (2500/80)	WT-E (2000/80)	WT-F (2750/92)
Months	kWh	kWh	kWh	kWh	kWh	kWh
1	2010084	1894697	3676810	1806572	2070948	2738829
2	2898261	2731889	3736381	2643763	2952202	3846015
3	2945007	2775951	3736381	2687826	2952202	3904288
4	6450968	6477220	7640063	6212844	6212844	8216486
5	10985343	11852872	11934113	11147869	10002238	13461051
6	9208990	9649736	10372640	9165046	8592231	11479771
7	11546297	12601938	12436015	11808809	10442865	14102054
8	7759860	7975353	8978468	7578788	7358475	9789856
9	8928513	9341297	10093806	8856607	8371917	11130133
10	2384053	2203136	8122945	2159073	2423450	3205012
11	1355638	1145631	1784540	1189693	1410007	1806461
12	2010084	1850634	2621043	1762509	2070948	2680556
Annual	68483098	70500354	85133205	67019399	64860327	86360512

TABLE 17: Wind turbine capacity factor for a period of one year.

Wind turbine	WT-A (2300/82.4)	WT-B (2750/80)	WT-C (2300/90)	WT-D (2500/80)	WT-E (2000/80)	WT-F (2750/92)
Months	CF	CF	CF	CF	CF	CF
1	10	8	13	8	12	11
2	14	11	19	12	17	16
3	15	12	19	12	17	16
4	32	27	38	28	35	34
5	54	49	59	51	57	56
6	46	40	51	42	49	48
7	57	52	62	54	60	58
8	38	33	45	35	42	41
9	44	39	50	40	48	46
10	12	9	15	10	14	13
11	7	5	09	5	8	7
12	10	8	13	8	12	11
Average (%)	28.25	24.41	32.75	25.41	30.91	29.75

$$E = T_{ah} \times R_p \times C_f,$$

$$E = \frac{1}{T_{ah}} \left(\frac{1}{R_p C_f} \right) \left[1 + n \left\{ \frac{(1 - i_r)^t - 1}{i_r (1 + i_r)^t} \right\} \right]. \quad (19)$$

To calculate the energy output, the considered investment cost of wind turbine is US \$1000/kW. The installation cost, operation cost, and interest rate is 20 %, 3 %, and 5 % of

the investment cost of wind turbine, respectively. The investment cost, installation cost, operation cost, and interest rate are taken from [48, 49][51, 52]. As per cost estimation of selected wind turbines, the wind turbine WT-C has lowest cost US\$ Cent 0.0346/kWh with lowest capacity factors of 0.3275 (32.75%). The economic assessment results show that the wind turbine WT-C has an edge over the other wind turbines in terms of price per kilowatt hour. Further, the details are given in Table 18.

TABLE 18: Economic assessment/kWh (US\$) energy generated by wind turbines.

Wind turbine	WT-A	WT-B	WT-C	WT-D	WT-E	WT-F
(US\$)	(2300/82.4)	(2750/80)	(2300/90)	(2500/80)	(2000/80)	(2750/92)
(Cost/kWh)	0.0430	0.050	0.0346	0.0480	0.0394	0.0400

5. Conclusions

In this paper, the wind resource and power assessment of Gharo site is assessed at three different measurement heights including 10, 30, and 50 m above the ground level. The wind characteristics showed the strong presence at different heights. The wind power density and energy density are estimated. The present study is dedicated to the probability distribution function and frequency of the wind speed of candidate site. Additionally, the wind characteristics and power potential of Gharo site are studied while using the wind measurements at 10, 30, and 50 m heights. The overall mean wind speeds are found to be 6.89, 5.85, and 3.85 m/s at 50, 30, and 10 m, respectively, with corresponding standard deviation values of 2.946, 2.489, and 2.040. The mean values of the Weibull k parameter are estimated as 2.946, 2.489, and 2.040 while those of scale parameter are estimated as 7.634, 6.465, and 4.180 m/s at 50, 30, and 10 m, respectively. The respective mean wind power and energy density values are found to be 118.3, 92.20, and 46.10 W/m² and 1036.6, 807.90, and 402.60 kWh/m². As per cost estimation of wind turbines, the wind turbine WT-C has the lowest cost US\$ Cents of 0.0346/kWh and highest capacity factors of 0.3278 (32.78%). Wind turbine WT-C is recommended for this site for the wind farm deployment due to high energy generation and minimum price of energy. The resource analysis shows that Gharo site has a good potential for the deployment of wind farms.

Abbreviations

AGL:	Above the ground level
NREL:	National Renewable Energy Laboratories
IEC:	International Electrotechnical Commission
CF:	Capacity factor
MTOE:	Million tons of oil equivalent
GDP:	Gross domestic product
AEDB:	Alternate Energy Development Board
PMD:	Pakistan Meteorological Department
WT:	Wind turbine
WPD:	Wind power density
Pdf:	Probability distribution function
ED:	Energy density
kWh:	Kilowatt per hour
GWh:	Gigawatts per hour
W/m ² :	Watt per meter
kWh/m ² :	Kilowatt hour per meter
R :	Coefficient of correlation
AP:	Actual power
RP:	Rated power
k :	Weibull shapeless parameter
c (m/s):	Weibull scale parameter (m/s)

V :	Wind speed
σ :	Standard deviation
P_w :	Present worth
N_{pw} :	Net present worth
I_r :	Interest rate
T_{ah} :	Total annual hours
W_p :	Wind power
Om:	Operation and maintenance
Tc:	Total cost.

Data Availability

The data used to support the findings of this study are available from the corresponding author upon request.

Conflicts of Interest

The author declares that there are no conflicts of interest.

References

- [1] F. Shaikh, Q. Ji, and Y. Fan, "The diagnosis of an electricity crisis and alternative energy development in Pakistan," *Renewable and Sustainable Energy Reviews*, vol. 52, pp. 1172–1185, 2015.
- [2] Z. H. Hulio and W. Jiang, "Assessment of the apparent performance characterization along with levelized cost of energy of wind power plants considering real data," *Energy Exploration & Exploitation*, vol. 36, no. 6, 2018.
- [3] S. H. Shami, J. Ahmad, R. Zafar, M. Haris, and S. Bashir, "Evaluating wind energy potential in Pakistan's three provinces, with proposal for integration into national power grid," *Renewable and Sustainable Energy Reviews*, vol. 53, pp. 408–421, 2016.
- [4] D. P. Dee, S. M. Uppala, A. J. Simmons et al., "ERA-Interim reanalysis: configuration and performance of the data assimilation system," *Quarterly Journal of the Royal Meteorological Society*, vol. 137, no. 656, pp. 553–597.
- [5] J. J. Danielson and D. B. Gesch, "Global multi-resolution terrain elevation data 2010 (GMTED2010)," U. S Geological Survey, Reston, Virginia, 2011.
- [6] T. Aukitino, M. G. M. Khan, and M. R. Ahmed, "Wind energy resource assessment for Kiribati with a comparison of different methods of determining Weibull parameters," *Energy Conversion and Management*, vol. 151, pp. 641–660, 2017.
- [7] Z. H. Hulio, W. Jiang, and S. Rehman, "Technical and economic assessment of wind power potential of Nooriabad, Pakistan," *Energy, Sustainability and Society*, vol. 7, no. 1, p. 35, 2017.
- [8] V. Katinas, M. Marčiukaitis, G. Gecevičius, and A. Markevičius, "Statistical analysis of wind characteristics based on Weibull methods for estimation of power generation in Lithuania," *Renewable Energy*, vol. 113, pp. 190–201, 2017.
- [9] M. H. Soulouknga, S. Y. Doka, N. Revanna, N. Djongyang, and T. C. Kofane, "Analysis of wind speed data and wind energy potential in Faya-Largeau, Chad, using Weibull distribution," *Renewable Energy*, vol. 121, pp. 1–8, 2018.
- [10] A. Mostafaeipour, A. Sedaghat, A. A. Dehghan-Niri, and V. Kalantar, "Wind energy feasibility study for city of Shahrabak in Iran," *Renewable and Sustainable Energy Reviews*, vol. 15, no. 6, pp. 2545–2556, 2011.
- [11] A. Mostafaeipour, "Feasibility study of harnessing wind energy for turbine installation in province of Yazd in Iran,"

- Renewable and Sustainable Energy Reviews*, vol. 14, no. 1, pp. 93–111, 2010.
- [12] A. Keyhani, M. Ghasemi-Varnamkhasi, M. Khanali, and R. Abbaszadeh, "An assessment of wind energy potential as a power generation source in the capital of Iran, Tehran," *Energy*, vol. 35, no. 1, pp. 188–201, 2010.
- [13] K. Mohammadi and A. Mostafaeipour, "Using different methods for comprehensive study of wind turbine utilization in Zarrineh, Iran," *Energy Conversion and Management*, vol. 65, pp. 463–470, 2013.
- [14] A. Mostafaeipour, A. Sedaghat, M. Ghalishooyan et al., "Evaluation of wind energy potential as a power generation source for electricity production in Binalood, Iran," *Renewable Energy*, vol. 52, pp. 222–229, 2013.
- [15] M. Mirhosseini, F. Sharifi, and A. Sedaghat, "Assessing the wind energy potential locations in province of Semnan in Iran," *Renewable and Sustainable Energy Reviews*, vol. 15, no. 1, pp. 449–459, 2011.
- [16] A. Teimourian, A. Bahrami, H. Teimourian, M. Vala, and A. Oraj Huseyniklioglu, "Assessment of wind energy potential in the southeastern province of Iran," *Energy Sources, Part A: Recovery, Utilization, and Environmental Effects*, vol. 42, no. 3, pp. 329–343, 2020.
- [17] A. Bahrami, A. Teimourian, C. O. Okoye, and N. Khosravi, "Assessing the feasibility of wind energy as a power source in Turkmenistan; a major opportunity for Central Asia's energy market," *Energy*, vol. 183, pp. 415–427, 2019.
- [18] A. Bahrami, A. Teimourian, C. O. Okoye, and H. Shiri, "Technical and economic analysis of wind energy potential in Uzbekistan," *Journal of Cleaner Production*, vol. 223, pp. 801–814, 2019.
- [19] M. A. Alam, J. P. Meyer, M. M. Alam, and S. Rehman, "Wind speed and power characteristics for Jubail industrial city, Saudi Arabia," *Renewable and Sustainable Energy Reviews*, vol. 52, pp. 1193–1204, 2015.
- [20] M. A. Baseer and J. P. Meyer, S. Rehman and M. M. Alam, "Wind power characteristics of seven data collection sites in Jubail, Saudi Arabia using Weibull parameters," *Renewable Energy*, vol. 102, pp. 35–49, 2017.
- [21] M. A. Baseer, S. Rehman, J. P. Meyer, and M. M. Alam, "GIS-based site suitability analysis for wind farm development in Saudi Arabia," *Energy*, vol. 141, pp. 1166–1176, 2017.
- [22] M. Bassyouni, S. A. Gutub, U. Javaid et al., "and analysis of wind power resource using Weibull parameters," *Energy Exploration & Exploitation*, vol. 33, no. 1, pp. 105–122, 2015.
- [23] S. Rehman, "Wind energy resources assessment for Yanbo, Saudi Arabia," *Energy Conversion and Management*, vol. 45, no. 13–14, pp. 2019–2032, 2004.
- [24] S. Rehman, A. M. Mahbub Alam, J. P. Meyer, and L. M. Al-Hadhrani, "Wind speed characteristics and resource assessment using Weibull parameters," *International Journal of Green Energy*, vol. 9, no. 8, pp. 800–814, 2012.
- [25] S. Rehman, M. A. Mohandes, and L. M. Alhems, "Wind speed and power characteristics using LiDAR anemometer based measurements," *Sustainable Energy Technologies and Assessments*, vol. 27, pp. 46–62, 2018.
- [26] N. M. Al-Abadi and M. Naif, "Wind energy resource assessment for five locations in Saudi Arabia," *Renewable Energy*, vol. 30, no. 10, pp. 1489–1499, 2005.
- [27] M. Rafique, S. Rehman, M. Alam, and L. Alhems, "Feasibility of a 100 MW installed capacity wind farm for different climatic conditions," *Energies*, vol. 11, no. 8, p. 2147, 2018.
- [28] M. Li and X. Li, "Investigation of wind characteristics and assessment of wind energy potential for Waterloo region, Canada," *Energy Conversion and Management*, vol. 46, no. 18–19, pp. 3014–3033, 2005.
- [29] A. W. Dahmouni, M. Ben Salah, F. Askri, C. Kerkeni, and S. Ben Nasrallah, "Assessment of wind energy potential and optimal electricity generation in Borj-Cedria, Tunisia," *Renewable and Sustainable Energy Reviews*, vol. 15, no. 1, pp. 815–820, 2011.
- [30] H. Shafeek, I. E. Abbassi, A. E. Bouardi, and A. Darcherif, "Wind speed data analysis using Weibull and Rayleigh distribution functions, case study: five cities northern Morocco," *Procedia Manufacturing*, vol. 32, pp. 786–793, 2019.
- [31] A. Lashin and A. Shata, "An analysis of wind power potential in Port Said, Egypt," *Renewable and Sustainable Energy Reviews*, vol. 16, no. 9, pp. 6660–6667, 2012.
- [32] Y. Himri, S. Rehman, A. Agus Setiawan, and S. Himri, "Wind energy for rural areas of Algeria," *Renewable and Sustainable Energy Reviews*, vol. 16, no. 5, pp. 2381–2385, 2012.
- [33] Y. Himri, S. Rehman, S. Himri, K. Mohammadi, B. Sahin, and A. S. Malik, "Investigation of wind resources in Timimoun region, Algeria," *Wind Engineering*, vol. 40, no. 3, pp. 250–260, 2016.
- [34] Ž. Beljaars and J. Mikulović, "Assessment of the wind energy resource in the South Banat region, Serbia," *Renewable and Sustainable Energy Reviews*, vol. 16, no. 5, pp. 3014–3023, 2012.
- [35] M. E. Lee, G. Kim, S.-T. Jeong, and D. H. Ko, K. S. Kang, "Assessment of offshore wind energy at Younggwang in Korea," *Renewable and Sustainable Energy Reviews*, vol. 21, pp. 131–141, 2013.
- [36] J. Wu, J. Wang, and D. Chi, "Wind energy potential assessment for the site of Inner Mongolia in China," *Renewable and Sustainable Energy Reviews*, vol. 21, pp. 215–228, 2013.
- [37] M. Irwanto, N. Gomesh, M. R. Mamat, and Y. M. Yusoff, "Assessment of wind power generation potential in Perlis, Malaysia," *Renewable and Sustainable Energy Reviews*, vol. 38, pp. 296–308, 2014.
- [38] S. S. Chandhel, P. Ramasamy, and K. S. R. Murthy, "Wind power potential assessment of 12 locations in western Himalayan region of India," *Renewable and Sustainable Energy Reviews*, vol. 39, pp. 530–545, 2014.
- [39] A. S. Ahmed, "Potential wind power generation in South Egypt," *Renewable and Sustainable Energy Reviews*, vol. 16, no. 3, pp. 1528–1536, 2012.
- [40] A. K. Azad, M. G. Rasul, R. Islam, and I. R. Shishir, "Analysis of wind energy prospect for power generation by three Weibull distribution methods," *Energy Procedia*, vol. 75, pp. 722–727, 2015.
- [41] Z. H. Hulio, W. Jiang, and S. Rehman, "Techno - economic assessment of wind power potential of Hawke's Bay using Weibull parameter: a review," *Energy Strategy Reviews*, vol. 26, p. 100375, 2019.
- [42] G. V. Ochoa, J. N. Alvarez, and M. V. Chamorro, "Data set on wind speed, wind direction and wind probability distributions in Puerto Bolivar-Colombia," *Data in Brief*, vol. 27, p. 104753, 2019.
- [43] Z. H. Hulio and W. Jiang, "An assessment of effects of non-stationary operational conditions on wind turbine under different wind scenario," *Journal of Engineering, Design and Technology*, vol. 18, no. 1, 2019.
- [44] E. K. Akpınar and S. Akpınar, "An assessment on seasonal analysis of wind energy characteristics and wind turbine characteristics," *Energy Conversion and Management*, vol. 46, no. 11–12, pp. 1848–1867, 2005.

- [45] M. Gökçek, A. Bayülken, and Ş. Bekdemir, "Investigation of wind characteristics and wind energy potential in Kırklareli, Turkey," *Renewable Energy*, vol. 32, no. 10, pp. 1739–1752, 2007.
- [46] B. Yaniktepe, T. Koroglu, and M. M. Savrun, "Investigation of wind characteristics and wind energy potential in Osmaniye, Turkey," *Renewable and Sustainable Energy Reviews*, vol. 21, pp. 703–711, 2013.
- [47] Z. H. Hulio and W. Jiang, "Wind energy potential assessment for KPT with a comparison of different methods of determining Weibull parameters," *International Journal of Energy Sector Management*, vol. 14, no. 1, 2019.
- [48] J. Wei, Z. H. Hulio, and H. Rashid, "Site specific assessment of wind characteristics and determination of wind loads effects on wind turbine components and energy generation," *International Journal of Energy Sector Management*, vol. 12, no. 3, 2018.
- [49] Z. H. Hulio and W. Jiang, "Site specific technical and economic analysis of wind power potential and energy generation using Weibull parameters," *World Journal of Science, Technology and Sustainable Development*, vol. 15, no. 1, 2017.
- [50] A. Ucar and F. Balo, "Evaluation of wind energy potential and electricity generation at six locations in Turkey," *Applied Energy*, vol. 86, no. 10, pp. 1864–1872, 2009.
- [51] Danish Wind Turbine Manufacturers Association, *Guided Tour on Wind Energy*, Danish Wind Turbine Manufacturers Association, Copenhagen, Denmark, 1999.
- [52] I. Ullah, Q.-U.-Z. Chaudhry, and A. J. Chipperfield, "An evaluation of wind energy potential at Kati Bandar, Pakistan," *Renewable and Sustainable Energy Reviews*, vol. 14, no. 2, pp. 856–861, 2010.